

Primordial Gravitational Wave Background as a Probe of the Primordial Black Holes

Utkarsh Kumar ^{1,*}

¹*Department of Physics, University of Ottawa, Ottawa, ON K1N6N5, Canada*

(Dated: Tuesday 15th July, 2025)

We study the formation of primordial black holes (PBHs) from the collapse of density perturbations induced by primordial gravitational waves (PGWs). The PGWs' interpretation of the stochastic gravitational wave background (SGWB) detected by the Pulsar Timing Array (PTA) corresponds to PBHs formation in the mass range $[10^{-12} - 10^{-3}]M_{\odot}$. Importantly, our analysis shows that PGWs' interpretation of recent PTA data remains viable, as it does not lead to PBH overproduction. We derive the amplitude of PGWs by leveraging existing constraints on the PBH abundance across a wide mass range. Notably, these constrained amplitudes predict SGWB signals that would be detectable by future gravitational wave observatories.

Introduction– The various detections of gravitational waves (GWs) from binary black holes (BBHs) [1–5] and a binary neutron star (BNS) [6] by LIGO/Virgo have prompted interest in the physics of Primordial Black Holes (PBHs) [7–10]. The PBH scenario is intriguing because it can explain the event rate of LIGO/Virgo BBHs and account for all dark matter [11–30]. There are several mechanisms for the formation of these PBHs, and their masses span a wide range of values [31–33]. In the standard scenario, PBHs can form due to enhanced primordial curvature perturbations at small scales created by inflation in the very early Universe. These same curvature fluctuations can source tensor modes at second order in perturbation theory [34–56]. Consequently, PBH formation in this case inevitably leads to scalar-induced gravitational waves (SIGWs). Recent pulsar timing array (PTA) experiments, including NANOGrav [57, 58], CPTA [59], PPTA [60], and EPTA+InPTA [61, 62], have shown evidence for the existence of a stochastic background of GWs (SGWB). If this observed SGWB is interpreted as SIGWs, it allows us to estimate the abundance of PBHs. Other possible sources of the observed SGWB, including phase transitions [63–67] that cause bubble collisions, cosmic string formation [68–71], and domain wall formation [72, 73], can produce populations of PBHs, except for primordial GWs (PGWs) [74–91].

In this paper, we explore an alternative approach to probe the PBH scenario in which PGWs act as a source for generating second-order radiation-density perturbations. This mechanism has been considered previously to study the generation and evolution of matter-density perturbations, quantifying the impact of PGWs on the Large-Scale Structure of the Universe [92–97]. Here, we focus on smaller scales relevant to current PTA data releases and next-generation gravitational wave interferometers, such as LISA [98], DECIGO [99], μ Ares [100], and future LISA-type missions [101, 102].

The goal of this paper is to demonstrate that small-scale PGWs can produce PBHs across various mass windows. We focus specifically on inflation models where

the linear power spectrum is either a power-law or has a log-normal shape, as predicted by several inflationary scenarios [103–107]. We show that the PGW interpretation of NANOGrav and EPTA DR2 results is associated with PBH formation, with the mass function falling within $[10^{-12} - 10^{-3}]M_{\odot}$. Additionally, our approach provides a framework to constrain tensor-mode amplitude by leveraging existing limits on PBH abundances set by evaporation [108], gravitational lensing [109–119], dynamical effects [29, 120–125].

PGWs induced density perturbations We consider the spatially flat Friedmann-Lemaître-Robertson-Walker (FLRW) spacetime perturbed up to second order with negligible anisotropic stress

$$ds^2 = a(\eta)^2 [-d\eta^2 + \gamma_{ij}(x, \eta) dx^i dx^j], \quad (1)$$

where $a(\eta)$ is the scale factor in conformal time and γ_{ij} is the conformal spatial metric containing scalar and tensor perturbations at first and second order. At second order γ_{ij} is defined as: $(1 - \phi^{(2)})\delta_{ij} + (1/2)(\partial_i\partial_j - (1/3)\nabla^2\delta_{ij})\chi^{\parallel(2)} + \chi_{ij}^{(1)T}$ with $\chi_{ij}^{(1)T}$ being first-order tensor modes and $\phi^{(2)}$ and $\chi^{\parallel(2)}$ are tensor induced scalar perturbations. We assume the Universe is filled with a radiation fluid whose large overdensities collapse after the horizon entry, leading to the formation of PBHs. The evolution equations for second-order density ($\delta^{(2)}$) and velocity ($v^{(2)}$) perturbations are:

$$\begin{aligned} \delta^{(2)'} + \frac{4}{3}\nabla^2 v^{(2)} - 4\phi^{(2)'} &= \frac{4}{3}\chi^{(1)ij}\chi_{ij}^{(1)'}, \\ \delta^{(2)} + 4v^{(2)'} &= 0. \end{aligned} \quad (2)$$

Here, primes denote the derivatives with respect to conformal time, and \mathcal{H} is the conformal Hubble parameter. The evolution of $\phi^{(2)}$ is governed by the Einstein equations (time-time, time-space, and space-space components) [96]. Linear GWs ($\chi_{ij}^{(1)} \equiv \chi_{ij}$) evolve as:

$$\chi_{ij}'' + 2\mathcal{H}\chi_{ij}' - \nabla^2\chi_{ij} = 0 \quad (3)$$

The first-order tensor perturbation $\chi_{ij}(\mathbf{x}, \eta)$ is decomposed in Fourier space as

$$\chi_{ij}(\mathbf{x}, \eta) = \sum_{\sigma} \int \frac{d^3\mathbf{k}}{(2\pi)^{3/2}} e^{i\mathbf{k}\cdot\mathbf{x}} \chi_{\sigma}(\mathbf{k}, \eta) \epsilon_{ij}^{\sigma}(\hat{\mathbf{k}}) \quad (4)$$

* utkarshkumar.physics@gmail.com

where $\epsilon_{ij}^\sigma(\hat{\mathbf{k}})$ are the two polarization tensors ($\sigma = +, \times$) satisfying $\epsilon_{ij}^\sigma(\hat{\mathbf{k}})\epsilon^{\sigma'ij}(\hat{\mathbf{k}}) = 2\delta_{\sigma\sigma'}$, and $\chi_\sigma(\mathbf{k}, \eta)$ are the GW modes sourcing the density fluctuations. The temporal evolution of $\chi_\sigma(\mathbf{k}, \eta)$ can be decomposed into its primordial value and a transfer function [35, 96] as $\chi_\sigma(\mathbf{k})\sqrt{\pi/2x}J_{1/2}(x)$, where $J_{1/2}(x \equiv k\eta)$ is the Bessel function of order 1/2. The Fourier modes of density and velocity perturbations are also given in a similar fashion without the polarization tensors.

Combining Eq. (2) with Einstein equations yields the velocity fluctuation evolution in Fourier space:

$$v^{(2)'''} + \mathcal{H}v^{(2)''} - \left[4\mathcal{H}^2 - \frac{1}{3}k^2\right]v^{(2)'} + \frac{\mathcal{H}}{3}k^2v^{(2)} = \mathcal{S}. \quad (5)$$

Here, $\mathcal{S}(k, \eta)$ is the Fourier transform of $-\frac{1}{6}\chi^{ij'}\chi_{ij}'$. It is important to note that the LHS of Eq. (5) reduces to the linear velocity perturbation evolution when the source term \mathcal{S} vanishes. The solution of Eq. (5) is obtained, by transformation of $v^{(2)}$ to $u^{(2)} = (av^{(2)})'/a$, using the Green's function method. The tensor-induced density contrast $\delta^{(2)}(\eta, k)$ takes the following form:

$$\delta^{(2)}(\eta, k) = -\frac{\pi}{12} \sum_{\sigma, \sigma'} \int \frac{d^3\mathbf{q}}{(2\pi)^{3/2}} \epsilon_{ij}^\sigma(\hat{\mathbf{q}}) \epsilon^{\sigma'ij}(\widehat{\mathbf{k}-\mathbf{q}}) \left(\frac{q}{k} \frac{|\mathbf{k}-\mathbf{q}|}{k}\right)^{-1/2} \mathcal{I}(x, q, |\mathbf{k}-\mathbf{q}|) \chi^\sigma(\mathbf{k}) \chi^{\sigma'}(\mathbf{k}-\mathbf{q}) \quad (6)$$

The power spectrum of density perturbations induced by primordial tensors follows from the equal-time two-point correlators defined as

$$\langle \delta^{(2)}(\eta, \mathbf{k}) \delta^{(2)}(\eta, \mathbf{k}') \rangle = \delta^{(3)}(\mathbf{k} + \mathbf{k}') \frac{2\pi^2}{k^3} \mathcal{P}_{\delta^{(2)}}(\eta, \mathbf{k}). \quad (7)$$

Using Eqs. (6) and (7), the dimensionless power spectrum $\mathcal{P}_{\delta^{(2)}}(\eta, \mathbf{k})$ is computed as following:

$$\mathcal{P}_{\delta^{(2)}} = \frac{1}{2} \int_0^\infty dv \int_{|1-v|}^{1+v} \frac{f(u, v)}{(uv)^3} \overline{\mathcal{I}^2(u, v)} \mathcal{P}_\chi(ku) \mathcal{P}_\chi(kv) \quad (8)$$

Here $f(u, v)$ contracts the polarization tensors [95]. We employ a change of variables namely $v = \mathbf{q}/\mathbf{k}$, $u = |\mathbf{k}-\mathbf{q}|/\mathbf{k}$ and $x = \mathbf{k}\eta$ to arrive at the above form of $\mathcal{P}_{\delta^{(2)}}(\eta, \mathbf{k})$ in Eq. (8). The kernel $\mathcal{I}(x, u, v)$ constitutes the following time integrals of the product of three Bessel functions

$$\begin{aligned} \mathcal{I}_a(x, u, v) &= \int_0^x d\bar{x} \bar{x}^{-1/2} J_{3/2}\left(\frac{\bar{x}}{\sqrt{3}}\right) J_{3/2}(v\bar{x}) J_{3/2}(u\bar{x}) \\ \mathcal{I}_b(x, u, v) &= \int_0^x d\bar{x} \bar{x}^{-1/2} Y_{3/2}\left(\frac{\bar{x}}{\sqrt{3}}\right) J_{3/2}(v\bar{x}) J_{3/2}(u\bar{x}) \end{aligned} \quad (9)$$

These integrals should be evaluated for any values of x but the exact form of Eq. (9) is analytically obscure without giving a clear idea of time dependence. However, we can obtain the analytical formula for the integrals for the

scales leaving sub-horizon ($x \gg 1$) by extrapolating the upper limits of integrals to infinity [126–128]. We have explicitly checked this approximation using the numerical integral methods. The final form of time-average of kernel becomes $\overline{\mathcal{I}^2(u, v)} = \frac{\pi^3}{144} [\mathcal{I}_a^2(u, v) + \mathcal{I}_b^2(u, v)]$, with

$$\begin{aligned} \mathcal{I}_a(u, v) &= \frac{3^{3/4}}{2} \sqrt{\frac{2uv}{\pi}} (1-y^2) \Theta\left(u+v-\frac{1}{\sqrt{3}}\right) \\ \mathcal{I}_b(u, v) &= \frac{3^{3/4}}{2\pi} \sqrt{\frac{2uv}{\pi}} \left[y + \frac{(1-y^2)}{2} \log\left(\frac{1+y}{1-y}\right) \right] \end{aligned} \quad (10)$$

where $y = (u^2 + v^2 - 1/3)/(2uv)$. As shown in Eq. (8), the primordial tensor power spectrum influences the spectral shape of tensor-induced density perturbations irrespective of the GW source. In this work, we restrict ourselves to PGWs only. This primordial tensor power spectrum not only sources the second-order density power spectrum (leading to PBH formation) but also generates the SGWB observed by NANOGrav and other PTAs. In the following, we consider several ansätze for the tensor power spectrum, each with a distinct spectral shape applicable to different classes of models.

We first consider the typical power-law spectrum with pivot scale $k_s = 0.05 \text{Mpc}^{-1}$ predicted by single-field inflationary models [89, 129, 130]

$$\mathcal{P}_h^{\text{PL}}(k) = r A_s \left(\frac{k}{k_s}\right)^{n_T} \Theta(k_{\text{max}} - k). \quad (11)$$

where r is the tensor-to-scalar ratio with an upper bound $r \leq 0.032$ inferred from the joint analysis of Planck and BICEP/Keck [90], $A_s = 2.1 \times 10^{-9}$ is the amplitude of curvature perturbations measured at k_s [131], and n_T denotes the spectral tilt. Another class of spectra is characterized by a log-normal(LN) shape predicted by hybrid inflation and curvaton models [13, 19, 132]

$$\mathcal{P}_h^{\text{LN}}(k) = \frac{A_T}{\sqrt{2\pi}\Delta} \exp\left(-\frac{1}{2\Delta^2} \ln^2(k/k_p)\right), \quad (12)$$

where A_T is amplitude, k_p is peak of frequency, and Δ is width of LN spectrum. The present-day spectrum of GW energy density fraction is given by [133]

$$h^2 \Omega_{\text{GW}}(k) = \frac{\Omega_r^0 h^2}{24} \mathcal{P}_h(k), \quad (13)$$

where $\Omega_r^0 h^2 \simeq 4.2 \times 10^{-5}$ is the current energy density. The current GW frequency corresponds to $k = 6.25 \times 10^5 \text{Mpc}^{-1}$ (f/nHz). Furthermore, the GW energy spectrum contributes to the effective number of relativistic degrees of freedom parameterized by N_{eff} defined as [88, 89, 133–136]

$$\int_{f_{\text{BBN}}}^{f_{\text{max}}} \frac{df}{f} \Omega_{\text{GW}}(f) h^2 \leq 5.6 \times 10^{-6} \Delta N_{\text{eff}}. \quad (14)$$

Here, ΔN_{eff} represents the deviation from its standard model value. The frequency corresponding to the time of

the BBN era is $f_{\text{BBN}} = 1.84 \times 10^{-11}$ Hz. The upper limit of Eq. (14) is then fixed so that observational bounds on ΔN_{eff} are not violated. The 2σ upper limit on ΔN_{eff} is constrained by BBN and CMB probes to be $\Delta N_{\text{eff}} \leq 0.4$. [131, 137–142].

	Param	Prior	NG-15	EPTA2	NG-15 +EPTA2
PL	$\log_{10} r$	$[-40, -1]$	-9.5 ± 2.8	$-8.1^{+5.6}_{-2.5}$	-8.8 ± 2.5
	n_t	$[0, 4]$	1.91 ± 0.36	$1.73^{+0.31}_{-0.71}$	1.83 ± 0.31
LN	$\log_{10} A_T$	$[-10, 0]$	$-0.88^{+0.67}_{-0.46}$	$-1.33^{+0.85}_{-0.66}$	$-0.93^{+0.68}_{-0.46}$
	Δ	$[0.01, 4]$	$1.42^{+0.26}_{-0.53}$	$2.7^{+1.1}_{-1.4}$	$1.44^{+0.24}_{-0.54}$
	$\log_{10} f_p$	$[-10, -2]$	$-6.73^{+0.54}_{-0.76}$	$-6.2^{+1.4}_{-1.6}$	$-6.73^{+0.37}_{-0.94}$

TABLE I. Prior and mean $\pm 1\sigma$ constraints for power-law (PL) and log-normal (LN) spectra for NANOGrav-15, EPTA DR2, and their combination.

PBH formation: The PBHs are formed when the gravitational collapse of density perturbation $\delta(\eta, \mathbf{k})$ exceeds a critical threshold δ_c . Since the first-order tensor and first-order scalar modes are statistically independent, the total density contrast $\delta(\eta, \mathbf{k})$ upto second order is computed by simply adding both contributions as

$$\delta(\eta, \mathbf{k}) = \frac{4}{9} \frac{k^2}{\mathcal{H}^2} \mathcal{T}(\eta, \mathbf{k}) \zeta^{(1)}(\mathbf{k}) + \delta^{(2)}(\eta, \mathbf{k}) \quad (15)$$

Here we have related the first-order density perturbation $\delta^{(1)}(\eta, \mathbf{k})$ to the first-order primordial curvature perturbation $\zeta^{(1)}(\mathbf{k})$ via a transfer function $\mathcal{T}(\eta, \mathbf{k})$. Given that the first-order curvature perturbations are scale-invariant and their amplitude is tightly constrained at large scales using the Planck’s CMB measurements, the contribution of linear modes in Eq. (15) is sub-dominant. However tensor-induced density perturbations start to dominate at small scales. We adopt the Press–Schechter formalism [143, 144] to compute the fraction of the density collapse to form PBHs, β is given by

$$\beta(M) = \int_{\delta_c}^{\infty} P(\delta) d\delta \equiv \frac{1}{2} \operatorname{erfc} \left\{ \frac{\delta_c}{\sqrt{2} \sigma_{\delta}(M)} \right\}, \quad (16)$$

The above relation assumes that the probability distribution of density perturbation, $P(\delta)$, is Gaussian. In principle, the induced density contrast can be non-Gaussian due to its quadratic dependence on the primordial tensor perturbation. We leave the analysis including the ineludible non-Gaussianity for future work. The variance in the density fluctuations smoothed over a radius R using the Gaussian window function [154] $W(k, R) = \exp(-k^2 R^2/2)$, denoted as σ_{δ}^2 , obtained from

$$\sigma_{\delta}^2(M) = \int_0^{\infty} \frac{dk}{k} \mathcal{P}_{\delta}(k, \eta = R) W^2(k, R) \quad (17)$$

where M is the PBH mass and $R = 1/k(M)$ is smoothing scale for the PBH formation. The current fraction of

PBHs as DM over a logarithmic interval is

$$f_{\text{PBH}}(M) = \frac{1}{\Omega_{\text{DM}}} \frac{d\Omega_{\text{DM}}}{d \ln M} \simeq \frac{\beta(M)}{1.84 \times 10^{-8}} \left(\frac{M}{M_{\odot}} \right)^{-1/2}. \quad (18)$$

Finally, the mass of PBH is related to the scale of perturbation for PBH production as [155]

$$M_{\text{PBH}} \simeq M_{\odot} \left(\frac{\gamma}{0.2} \right) \left(\frac{g}{10.75} \right)^{-\frac{1}{6}} \left(\frac{k}{1.9 \times 10^5 \text{Mpc}^{-1}} \right)^{-2}. \quad (19)$$

where $\gamma = 0.2$ is the fraction of PBH mass in the horizon mass at the production [10], and $g = 10.75$ is the effective degrees of freedom for radiation at that time. We fix $\delta_c = 0.42$ for the computation of PBH abundance [31].

Analysis and results: We perform a joint Bayesian analysis of the NANOGrav15 (NG15) and EPTA DR2 (EPTA2) datasets. The joint constraints are derived by reweighting the NG15 chain samples, generated using PTArcade[156], based on posterior densities estimated from the EPTA2 chains via Gaussian Kernel Density Estimation. We then resample the full NG15 chain according to these computed weights. We use the publicly available tool GetDist[157] for analyzing chains. The prior information and mean $\pm 1\sigma$ constraints for both models are given in Table I. The two-dimensional contour plots for the inferred posterior values for PL and LN scenarios are shown in the left and right panels of Fig. 1 respectively. The dashed curves in the left panel of Fig. 1 represent contours of $\Delta N_{\text{eff}} = 0.4$ for different values of the reheating temperature T_{rh} . These contours consequently determine the k_{max} values appearing in Eqs. (11) and (14). The inference of blue spectrum and corresponding reheating temperatures required to fulfill ΔN_{eff} bound also has interesting consequences for formation of PBHs induced from the tensor modes. The blue spectral index of the PL spectrum provides the rise of the tensor-induced density power spectrum while reheating temperature fixes its peak (*see supplementary material*). The solid curves show the constraints on the spectral index (n_t) and $h^2 \Omega_{\text{GW}}(f_{\text{yr}})$ avoiding the overproduction of PBHs. The PL GW interpretation of the PTA signal in red survives but cannot account for the dark matter. The each isocontours of $f_{\text{pbh}} = 1$ corresponds to same f_{max} allowed to satisfy the N_{eff} constraints. It is important to note that for reheating temperatures as low as 5.05 GeV the whole parameter space is compatible with the PTA observations and also avoids the overproduction of the PBHs. It is striking to see from the Table I (*and also from full posterior distributions in supplementary material*) that NG15 offers stringent constraints compared to EPTA2 for LN specifically. We again show the allowed values of A_T for different values of Δ spread over the mean $\pm 1\sigma$ constraints satisfying $f_{\text{pbh}} = 1$ and $N_{\text{eff}} = 0.3$. See the SM for the evolution of the density power spectrum for the LN scenario.

The left panel of Fig. 2 displays the gravitational wave spectra for power-law (PL, orange) and log-normal (LN,

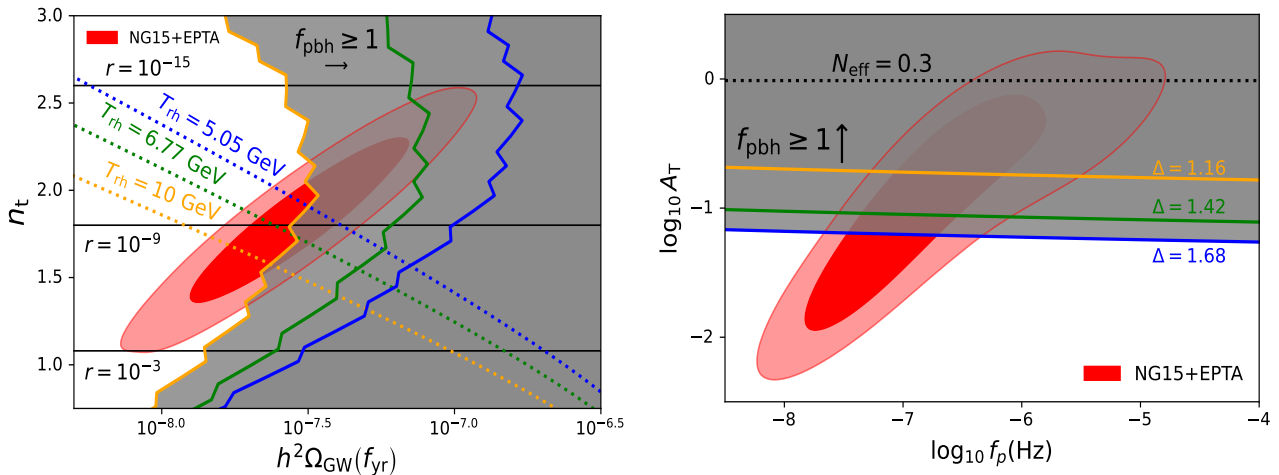


FIG. 1. *Left panel:* Two dimensional contour plot for inferred posterior values of n_t and present day GW energy density evaluated at reference frequency f_{yr} obtained from the joint analysis of NG-15 and EPTA-DR2 datasets. Black dashed curves correspond to the tensor-to-scalar ratio as shown. We include the allowed values of reheating temperatures that satisfy the N_{eff} bound (shown in dotted lines) and the corresponding viable parameter space (on the left) to avoid the overproduction of PBHs, given that $f_{\text{PBH}} \geq 1$. *Right panel:* same as left panel but for the LN model. Again, $N_{\text{eff}} = 0.3$ constraint given in black dashed line. The parameter space lying below blue ($\Delta = 1.68$), green ($\Delta = 1.42$), and orange ($\Delta = 1.16$) respectively survives the $f_{\text{PBH}} \geq 1$.

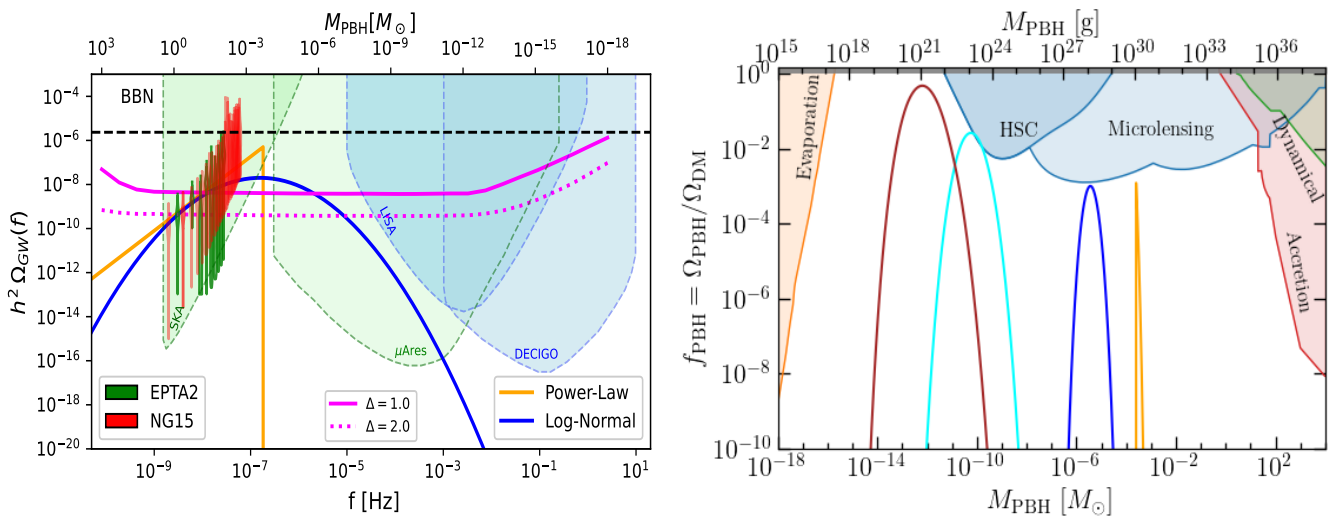


FIG. 2. *Left panel:* GW power spectra obtained from PL and LN spectra in orange and blue respectively. Shown are the violin plots in green and red for EPTA2 and NG15 measurements respectively, and the sensitivity curves for SKA, μAres , LISA, and DECIGO in colors indicated. *Right panel:* Mass function resulting from the PL (orange) and LN spectrum for the values of parameters described in the text. The PBHs abundance constrained by variety of observations including PBH evaporation[108, 145–153], gravitational lensing[109–119], dynamical effects[29, 120–125] are also shown.

blue) models, using parameters within the 1σ confidence region from joint PTA analyses. For the PL spectrum, we adopt $r = 2.56 \times 10^{-8}$, $n_t = 1.68$, and $k_{\text{max}} = 1.2 \times 10^8 \text{ Mpc}^{-1}$ (corresponding to $T_{\text{rh}} = 10 \text{ GeV}$). The LN spectrum uses $A_T = 9.2 \times 10^{-2}$, $\Delta = 1.42$, and $\log_{10} f_p = -6.8$. These parameters yield PBH abundances of $10^{-3} M_\odot$ and $10^{-5} M_\odot$ for the PL and LN models, respectively. Tight constraints on k_{max} from ΔN_{eff} measurements limit the PL spectrum to PBH masses near

$10^{-3} M_\odot$ while simultaneously explaining both NG15 and EPTA datasets. In contrast, the LN model's PBH mass range is determined by the peak frequency f_p , allowing broader mass possibilities. As mentioned earlier, the EPTA2 has a wide parameter space that can account for the PBHs as dark matter. The mass function resulting from the 95% C.I. posterior values of the EPTA2 parameter space in cyan and brown color in right panel of Fig. 2. We overlay the corresponding parameter values in the

same color in SM (see right panel, Fig. S.3).

Constraints on $h^2\Omega_{\text{GW}}$ from f_{PBH} : Figs. 1 and 2 show that the f_{pbh} imposes additional constraints on inferred model parameters. The abundance of PBHs has been constrained by a variety of observations, including extra-galactic γ -rays from PBH evaporation[108, 145–153], femtolensing of γ -ray bursts [145], Subaru/HSC microlensing[158, 159], Kepler milli/microlensing [118], OGLE microlensing [109], EROS/MACHO microlensing[116]. Using these observational bounds, we derive the amplitude of the SGWB when interpreted as PGWs. For the LN spectrum, we compute the allowed values of A_{T} and consequently $h^2\Omega_{\text{GW}}$ at each peak frequency f_p consistent with f_{pbh} constraints. This analysis considers spectral width parameters $\Delta = 1.0$ and $\Delta = 2.0$, with the resulting SGWB spectra presented in the left panel of Fig. 2. Solid and dotted orange lines respectively denote the $\Delta = 1.0$ and $\Delta = 2.0$ cases. It is interesting to note that the derived $\Omega_{\text{GW}}(f_p)$ amplitudes fall within the sensitivity ranges of several next-generation gravitational wave observatories, indicating the inevitability of the production of PBHs from the PGWs.

Conclusions and outlook: In this paper, we have analyzed a novel mechanism for PBH formation from the collapse of radiation overdensities induced by first-order PGWs. PBH production in such a scenario occurs irrespective of the PGW source. Using Inflationary PGWs as a potential explanation for the observed SGWB, we per-

formed a joint log-likelihood analysis with NANOGrav and EPTA data. Our results demonstrate that PGWs can generate a sizable abundance of PBHs while simultaneously satisfying constraints from PBH overproduction and the NG15+EPTA datasets. Furthermore, our formalism provides a framework for assessing the detectability prospects of the PGW background, ensuring consistency with observational bounds on the PBH fraction (f_{pbh}) across a wide range of scales. We explicitly show that future missions, including SKA, LISA, and DECIGO, could produce PBHs acting as primordial seeds for supermassive black holes or potentially explain dark matter partially or entirely.

The present analysis can be extended in several ways. It has been shown in several previous works that computation of PBH abundances comes with many levels of uncertainties including the underlying theory, value of critical threshold, and choices of different types of window functions [160–162]. Future work could employ peak theory to calculate PBH abundance more precisely [163–165]. Moreover, we omitted contributions from the ineludible non-Gaussianity arising from quadratic tensor modes in the source term. Incorporating this effect, along with considering the inherent non-Gaussian statistics of PGWs, would be valuable[97, 166–168]. We expect a comprehensive analysis accounting for these considerations will further refine the parameter space inferred from current PTA results and enhance the detection prospects for upcoming missions.

-
- [1] B. P. Abbott *et al.* (LIGO Scientific, Virgo), *Phys. Rev. Lett.* **116**, 061102 (2016), arXiv:1602.03837 [gr-qc].
 - [2] B. P. Abbott *et al.* (LIGO Scientific, Virgo), *Phys. Rev. Lett.* **116**, 241103 (2016), arXiv:1606.04855 [gr-qc].
 - [3] B. P. Abbott *et al.* (LIGO Scientific, VIRGO), *Phys. Rev. Lett.* **118**, 221101 (2017), [Erratum: Phys.Rev.Lett. 121, 129901 (2018)], arXiv:1706.01812 [gr-qc].
 - [4] B. P. Abbott *et al.* (LIGO Scientific, Virgo), *Astrophys. J. Lett.* **851**, L35 (2017), arXiv:1711.05578 [astro-ph.HE].
 - [5] B. P. Abbott *et al.* (LIGO Scientific, Virgo), *Phys. Rev. Lett.* **119**, 141101 (2017), arXiv:1709.09660 [gr-qc].
 - [6] B. P. Abbott *et al.* (LIGO Scientific, Virgo), *Phys. Rev. Lett.* **119**, 161101 (2017), arXiv:1710.05832 [gr-qc].
 - [7] Y. B. Zel'dovich and I. D. Novikov, *Sov. Astron.* **10**, 602 (1967).
 - [8] S. Hawking, *Mon. Not. Roy. Astron. Soc.* **152**, 75 (1971).
 - [9] B. J. Carr and S. W. Hawking, *Mon. Not. Roy. Astron. Soc.* **168**, 399 (1974).
 - [10] B. J. Carr, *Astrophys. J.* **201**, 1 (1975).
 - [11] J. Garcia-Bellido, A. D. Linde, and D. Wands, *Phys. Rev. D* **54**, 6040 (1996), arXiv:astro-ph/9605094.
 - [12] M. Y. Khlopov, *Res. Astron. Astrophys.* **10**, 495 (2010), arXiv:0801.0116 [astro-ph].
 - [13] P. H. Frampton, M. Kawasaki, F. Takahashi, and T. T. Yanagida, *JCAP* **04**, 023 (2010), arXiv:1001.2308 [hep-ph].
 - [14] M. Kawasaki, A. Kusenko, Y. Tada, and T. T. Yanagida, *Phys. Rev. D* **94**, 083523 (2016), arXiv:1606.07631 [astro-ph.CO].
 - [15] E. Cotner and A. Kusenko, *Phys. Rev. Lett.* **119**, 031103 (2017), arXiv:1612.02529 [astro-ph.CO].
 - [16] E. Cotner and A. Kusenko, *Phys. Rev. D* **96**, 103002 (2017), arXiv:1706.09003 [astro-ph.CO].
 - [17] B. Carr, F. Kuhnel, and M. Sandstad, *Phys. Rev. D* **94**, 083504 (2016), arXiv:1607.06077 [astro-ph.CO].
 - [18] K. Inomata, M. Kawasaki, K. Mukaida, Y. Tada, and T. T. Yanagida, *Phys. Rev. D* **95**, 123510 (2017), arXiv:1611.06130 [astro-ph.CO].
 - [19] S. Pi, Y.-l. Zhang, Q.-G. Huang, and M. Sasaki, *JCAP* **05**, 042 (2018), arXiv:1712.09896 [astro-ph.CO].
 - [20] K. Inomata, M. Kawasaki, K. Mukaida, Y. Tada, and T. T. Yanagida, *Phys. Rev. D* **96**, 043504 (2017), arXiv:1701.02544 [astro-ph.CO].
 - [21] J. Garcia-Bellido, M. Peloso, and C. Unal, *JCAP* **09**, 013 (2017), arXiv:1707.02441 [astro-ph.CO].
 - [22] Y. Inoue and A. Kusenko, *JCAP* **10**, 034 (2017), arXiv:1705.00791 [astro-ph.CO].
 - [23] J. Georg and S. Watson, *JHEP* **09**, 138 (2017), arXiv:1703.04825 [astro-ph.CO].
 - [24] K. Inomata, M. Kawasaki, K. Mukaida, and T. T. Yanagida, *Phys. Rev. D* **97**, 043514 (2018), arXiv:1711.06129 [astro-ph.CO].
 - [25] B. Kocsis, T. Suyama, T. Tanaka, and S. Yokoyama, *Astrophys. J.* **854**, 41 (2018), arXiv:1709.09007 [astro-ph].

- ph.CO].
- [26] K. Ando, K. Inomata, M. Kawasaki, K. Mukaida, and T. T. Yanagida, *Phys. Rev. D* **97**, 123512 (2018), arXiv:1711.08956 [astro-ph.CO].
- [27] E. Cotner, A. Kusenko, and V. Takhistov, *Phys. Rev. D* **98**, 083513 (2018), arXiv:1801.03321 [astro-ph.CO].
- [28] M. Sasaki, T. Suyama, T. Tanaka, and S. Yokoyama, *Class. Quant. Grav.* **35**, 063001 (2018), arXiv:1801.05235 [astro-ph.CO].
- [29] B. Carr and J. Silk, *Mon. Not. Roy. Astron. Soc.* **478**, 3756 (2018), arXiv:1801.00672 [astro-ph.CO].
- [30] E. Cotner, A. Kusenko, M. Sasaki, and V. Takhistov, *JCAP* **10**, 077 (2019), arXiv:1907.10613 [astro-ph.CO].
- [31] B. Carr and F. Kuhnel, *Ann. Rev. Nucl. Part. Sci.* **70**, 355 (2020), arXiv:2006.02838 [astro-ph.CO].
- [32] A. M. Green and B. J. Kavanagh, *J. Phys. G* **48**, 043001 (2021), arXiv:2007.10722 [astro-ph.CO].
- [33] S. Bird *et al.*, *Phys. Dark Univ.* **41**, 101231 (2023), arXiv:2203.08967 [hep-ph].
- [34] D. Baumann, P. J. Steinhardt, K. Takahashi, and K. Ichiki, *Phys. Rev. D* **76**, 084019 (2007), arXiv:hep-th/0703290.
- [35] R. Picard and K. A. Malik, . (2023), arXiv:2311.14513 [astro-ph.CO].
- [36] G. Domènech, *Universe* **7**, 398 (2021), arXiv:2109.01398 [gr-qc].
- [37] P. Bari, N. Bartolo, G. Domènech, and S. Matarrese, *Phys. Rev. D* **109**, 023509 (2024), arXiv:2307.05404 [astro-ph.CO].
- [38] S. Balaji, G. Domènech, and G. Franciolini, *JCAP* **10**, 041 (2023), arXiv:2307.08552 [gr-qc].
- [39] G. Domènech, *AAPPS Bull.* **34**, 4 (2024), arXiv:2311.02065 [gr-qc].
- [40] Z.-C. Chen, J. Li, L. Liu, and Z. Yi, *Phys. Rev. D* **109**, L101302 (2024), arXiv:2401.09818 [gr-qc].
- [41] G. Domènech, S. Pi, A. Wang, and J. Wang, *JCAP* **08**, 054 (2024), arXiv:2402.18965 [astro-ph.CO].
- [42] G. Domènech and A. Ganz, . (2024), arXiv:2406.19950 [gr-qc].
- [43] K. D. Lozanov, M. Sasaki, and V. Takhistov, . (2023), arXiv:2304.06709 [astro-ph.CO].
- [44] K. D. Lozanov, M. Sasaki, and V. Takhistov, *Phys. Lett. B* **848**, 138392 (2024), arXiv:2309.14193 [astro-ph.CO].
- [45] K. D. Lozanov, S. Pi, M. Sasaki, V. Takhistov, and A. Wang, . (2023), arXiv:2310.03594 [astro-ph.CO].
- [46] P. Adshead, K. D. Lozanov, and Z. J. Weiner, *JCAP* **10**, 080 (2021), arXiv:2105.01659 [astro-ph.CO].
- [47] G. Domènech, S. Pi, and M. Sasaki, *JCAP* **08**, 017 (2020), arXiv:2005.12314 [gr-qc].
- [48] K. Inomata, K. Kohri, T. Nakama, and T. Terada, *JCAP* **10**, 071 (2019), [Erratum: *JCAP* **08**, E01 (2023)], arXiv:1904.12878 [astro-ph.CO].
- [49] Z.-Q. You, Z. Yi, and Y. Wu, *JCAP* **11**, 065 (2023), arXiv:2307.04419 [gr-qc].
- [50] S. A. Hosseini Mansoori, F. Felegray, A. Talebian, and M. Sami, *JCAP* **08**, 067 (2023), arXiv:2307.06757 [astro-ph.CO].
- [51] M. A. Gorji, M. Sasaki, and T. Suyama, *Phys. Lett. B* **846**, 138214 (2023), arXiv:2307.13109 [astro-ph.CO].
- [52] L. Liu, Z.-C. Chen, and Q.-G. Huang, *JCAP* **11**, 071 (2023), arXiv:2307.14911 [astro-ph.CO].
- [53] L. Frosina and A. Urbano, *Phys. Rev. D* **108**, 103544 (2023), arXiv:2308.06915 [astro-ph.CO].
- [54] S. Choudhury, A. Karde, S. Panda, and M. Sami, *Nucl. Phys. B* **1007**, 116678 (2024), arXiv:2308.09273 [astro-ph.CO].
- [55] K. Harigaya, K. Inomata, and T. Terada, *Phys. Rev. D* **108**, 123538 (2023), arXiv:2309.00228 [astro-ph.CO].
- [56] U. Kumar, U. Thattarampilly, and P. Chaturvedi, . (2024), arXiv:2410.12931 [astro-ph.CO].
- [57] G. Agazie *et al.* (NANOGrav), *Astrophys. J. Lett.* **951**, L8 (2023), arXiv:2306.16213 [astro-ph.HE].
- [58] Z. Arzoumanian *et al.* (NANOGrav), *Astrophys. J.* **859**, 47 (2018), arXiv:1801.02617 [astro-ph.HE].
- [59] H. Xu *et al.*, *Res. Astron. Astrophys.* **23**, 075024 (2023), arXiv:2306.16216 [astro-ph.HE].
- [60] D. J. Reardon *et al.*, *Astrophys. J. Lett.* **951**, L6 (2023), arXiv:2306.16215 [astro-ph.HE].
- [61] J. Antoniadis *et al.* (EPTA, InPTA:), *Astron. Astrophys.* **678**, A50 (2023), arXiv:2306.16214 [astro-ph.HE].
- [62] J. Antoniadis *et al.* (EPTA, InPTA), *Astron. Astrophys.* **685**, A94 (2024), arXiv:2306.16227 [astro-ph.CO].
- [63] T. Ghosh, A. Ghoshal, H.-K. Guo, F. Hajkarim, S. F. King, K. Sinha, X. Wang, and G. White, *JCAP* **05**, 100 (2024), arXiv:2307.02259 [astro-ph.HE].
- [64] T. Bringmann, P. F. Depta, T. Konstandin, K. Schmidt-Hoberg, and C. Tassilo, *JCAP* **11**, 053 (2023), arXiv:2306.09411 [astro-ph.CO].
- [65] Z. Arzoumanian *et al.* (NANOGrav), *Phys. Rev. Lett.* **127**, 251302 (2021), arXiv:2104.13930 [astro-ph.CO].
- [66] Y. Gouttenoire, *Phys. Rev. Lett.* **131**, 171404 (2023), arXiv:2307.04239 [hep-ph].
- [67] Z.-C. Chen, S.-L. Li, P. Wu, and H. Yu, *Phys. Rev. D* **109**, 043022 (2024), arXiv:2312.01824 [astro-ph.CO].
- [68] J. Ellis and M. Lewicki, *Phys. Rev. Lett.* **126**, 041304 (2021), arXiv:2009.06555 [astro-ph.CO].
- [69] S. Blasi, V. Brdar, and K. Schmitz, *Phys. Rev. Lett.* **126**, 041305 (2021), arXiv:2009.06607 [astro-ph.CO].
- [70] J. Ellis, M. Fairbairn, G. Franciolini, G. Hütsi, A. Iovino, M. Lewicki, M. Raidal, J. Urrutia, V. Vasikonen, and H. Veermäe, *Phys. Rev. D* **109**, 023522 (2024), arXiv:2308.08546 [astro-ph.CO].
- [71] R. Maji and W.-I. Park, *JCAP* **01**, 015 (2024), arXiv:2308.11439 [hep-ph].
- [72] Y. Gouttenoire and E. Vitagliano, . (2023), arXiv:2306.17841 [gr-qc].
- [73] Z. Zhang, C. Cai, Y.-H. Su, S. Wang, Z.-H. Yu, and H.-H. Zhang, *Phys. Rev. D* **108**, 095037 (2023), arXiv:2307.11495 [hep-ph].
- [74] I. Ben-Dayan, U. Kumar, U. Thattarampilly, and A. Verma, *Phys. Rev. D* **108**, 103507 (2023), arXiv:2307.15123 [astro-ph.CO].
- [75] S. Vagnozzi, *JHEAp* **39**, 81 (2023), arXiv:2306.16912 [astro-ph.CO].
- [76] M. Benetti, L. L. Graef, and S. Vagnozzi, *Phys. Rev. D* **105**, 043520 (2022), arXiv:2111.04758 [astro-ph.CO].
- [77] S. Vagnozzi and A. Loeb, *Astrophys. J. Lett.* **939**, L22 (2022), arXiv:2208.14088 [astro-ph.CO].
- [78] B. Das, N. Jaman, and M. Sami, *Phys. Rev. D* **108**, 103510 (2023), arXiv:2307.12913 [gr-qc].
- [79] S. Datta and R. Samanta, *Phys. Rev. D* **108**, L091706 (2023), arXiv:2307.00646 [hep-ph].
- [80] S. Vagnozzi, *Mon. Not. Roy. Astron. Soc.* **502**, L11 (2021), arXiv:2009.13432 [astro-ph.CO].
- [81] J. Antoniadis *et al.*, *Mon. Not. Roy. Astron. Soc.* **510**, 4873 (2022), arXiv:2201.03980 [astro-ph.HE].
- [82] S. Chen *et al.* (EPTA), *Mon. Not. Roy. Astron. Soc.*

- 508**, 4970 (2021), arXiv:2110.13184 [astro-ph.HE].
- [83] B. Goncharov *et al.*, *Astrophys. J. Lett.* **917**, L19 (2021), arXiv:2107.12112 [astro-ph.HE].
- [84] Z. Arzoumanian *et al.* (NANOGrav), *Astrophys. J. Lett.* **905**, L34 (2020), arXiv:2009.04496 [astro-ph.HE].
- [85] G. Hobbs and S. Dai, *Natl. Sci. Rev.* **4**, 707 (2017), arXiv:1707.01615 [astro-ph.IM].
- [86] A. I. Renzini, B. Goncharov, A. C. Jenkins, and P. M. Meyers, *Galaxies* **10**, 34 (2022), arXiv:2202.00178 [gr-qc].
- [87] I. Ben-Dayan, G. Calcagni, M. Gasperini, A. Mazumdar, E. Pavone, U. Thattarampilly, and A. Verma, *JCAP* **09**, 058 (2024), arXiv:2406.13521 [gr-qc].
- [88] I. Ben-Dayan, B. Keating, D. Leon, and I. Wolfson, *JCAP* **06**, 007 (2019), arXiv:1903.11843 [astro-ph.CO].
- [89] S. Kuroyanagi, T. Takahashi, and S. Yokoyama, *JCAP* **02**, 003 (2015), arXiv:1407.4785 [astro-ph.CO].
- [90] P. A. R. Ade *et al.* (BICEP, Keck), *Phys. Rev. Lett.* **127**, 151301 (2021), arXiv:2110.00483 [astro-ph.CO].
- [91] W. Giarè, M. Forconi, E. Di Valentino, and A. Melchiorri, *Mon. Not. Roy. Astron. Soc.* **520**, 2 (2023), arXiv:2210.14159 [astro-ph.CO].
- [92] K. Tomita, *Progress of Theoretical Physics* **45**, 1747 (1971), <https://academic.oup.com/ptp/article-pdf/45/6/1747/5306647/45-6-1747.pdf>.
- [93] K. Tomita, *Progress of Theoretical Physics* **47**, 416 (1972), <https://academic.oup.com/ptp/article-pdf/47/2/416/5280232/47-2-416.pdf>.
- [94] S. Matarrese, S. Mollerach, and M. Bruni, *Phys. Rev. D* **58**, 043504 (1998), arXiv:astro-ph/9707278.
- [95] P. Bari, A. Ricciardone, N. Bartolo, D. Bertacca, and S. Matarrese, *Phys. Rev. Lett.* **129**, 091301 (2022), arXiv:2111.06884 [astro-ph.CO].
- [96] P. Bari, D. Bertacca, N. Bartolo, A. Ricciardone, S. Giardiello, and S. Matarrese, *JCAP* **07**, 034 (2023), arXiv:2209.05329 [astro-ph.CO].
- [97] M. Abdelaziz, P. Bari, S. Matarrese, and A. Ricciardone, *Phys. Rev. D* **112**, 023505 (2025), arXiv:2504.07063 [astro-ph.CO].
- [98] P. Auclair *et al.* (LISA Cosmology Working Group), *Living Rev. Rel.* **26**, 5 (2023), arXiv:2204.05434 [astro-ph.CO].
- [99] S. Kawamura *et al.*, *PTEP* **2021**, 05A105 (2021), arXiv:2006.13545 [gr-qc].
- [100] A. Sesana *et al.*, *Exper. Astron.* **51**, 1333 (2021), arXiv:1908.11391 [astro-ph.IM].
- [101] W.-H. Ruan, Z.-K. Guo, R.-G. Cai, and Y.-Z. Zhang, *Int. J. Mod. Phys. A* **35**, 2050075 (2020), arXiv:1807.09495 [gr-qc].
- [102] S. Barke, Y. Wang, J. J. Esteban Delgado, M. Tröbs, G. Heinzel, and K. Danzmann, *Class. Quant. Grav.* **32**, 095004 (2015), arXiv:1411.1260 [physics.ins-det].
- [103] M. C. Guzzetti, N. Bartolo, M. Liguori, and S. Matarrese, *Riv. Nuovo Cim.* **39**, 399 (2016), arXiv:1605.01615 [astro-ph.CO].
- [104] E. Dimastrogiovanni, M. Fasiello, and T. Fujita, *JCAP* **01**, 019 (2017), arXiv:1608.04216 [astro-ph.CO].
- [105] B. Thorne, T. Fujita, M. Hazumi, N. Katayama, E. Komatsu, and M. Shiraiishi, *Phys. Rev. D* **97**, 043506 (2018), arXiv:1707.03240 [astro-ph.CO].
- [106] R. Namba, M. Peloso, M. Shiraiishi, L. Sorbo, and C. Unal, *JCAP* **01**, 041 (2016), arXiv:1509.07521 [astro-ph.CO].
- [107] A. Afzal, A. Ghoshal, and S. F. King, *Phys. Rev. D* **111**, 023050 (2025), arXiv:2407.15082 [astro-ph.CO].
- [108] B. J. Carr, K. Kohri, Y. Sendouda, and J. Yokoyama, *Phys. Rev. D* **81**, 104019 (2010), arXiv:0912.5297 [astro-ph.CO].
- [109] H. Niikura, M. Takada, S. Yokoyama, T. Sumi, and S. Masaki, *Phys. Rev. D* **99**, 083503 (2019), arXiv:1901.07120 [astro-ph.CO].
- [110] H. Niikura *et al.*, *Nature Astron.* **3**, 524 (2019), arXiv:1701.02151 [astro-ph.CO].
- [111] A. Barnacka, J. F. Glicenstein, and R. Moderski, *Phys. Rev. D* **86**, 043001 (2012), arXiv:1204.2056 [astro-ph.CO].
- [112] P. N. Wilkinson, D. R. Henstock, I. W. A. Browne, A. G. Polatidis, P. Augusto, A. C. S. Readhead, T. J. Pearson, W. Xu, G. B. Taylor, and R. C. Vermeulen, *Phys. Rev. Lett.* **86**, 584 (2001), arXiv:astro-ph/0101328.
- [113] M. Zumalacarregui and U. Seljak, *Phys. Rev. Lett.* **121**, 141101 (2018), arXiv:1712.02240 [astro-ph.CO].
- [114] M. Oguri, J. M. Diego, N. Kaiser, P. L. Kelly, and T. Broadhurst, *Phys. Rev. D* **97**, 023518 (2018), arXiv:1710.00148 [astro-ph.CO].
- [115] R. A. Allsman *et al.* (Macho), *Astrophys. J. Lett.* **550**, L169 (2001), arXiv:astro-ph/0011506.
- [116] P. Tisserand *et al.* (EROS-2), *Astron. Astrophys.* **469**, 387 (2007), arXiv:astro-ph/0607207.
- [117] K. Griest, A. M. Cieplak, and M. J. Lehner, *Astrophys. J.* **786**, 158 (2014), arXiv:1307.5798 [astro-ph.CO].
- [118] K. Griest, A. M. Cieplak, and M. J. Lehner, *Phys. Rev. Lett.* **111**, 181302 (2013).
- [119] N. Smyth, S. Profumo, S. English, T. Jeltema, K. McKinnon, and P. Guhathakurta, *Phys. Rev. D* **101**, 063005 (2020), arXiv:1910.01285 [astro-ph.CO].
- [120] P. W. Graham, S. Rajendran, and J. Varela, *Phys. Rev. D* **92**, 063007 (2015), arXiv:1505.04444 [hep-ph].
- [121] F. Capela, M. Pshirkov, and P. Tinyakov, *Phys. Rev. D* **87**, 123524 (2013), arXiv:1301.4984 [astro-ph.CO].
- [122] F. Capela, M. Pshirkov, and P. Tinyakov, *Phys. Rev. D* **87**, 023507 (2013), arXiv:1209.6021 [astro-ph.CO].
- [123] M. A. Monroy-Rodríguez and C. Allen, *Astrophys. J.* **790**, 159 (2014), arXiv:1406.5169 [astro-ph.GA].
- [124] S. L. Zoutendijk *et al.* (MUSE), *Astron. Astrophys.* **635**, A107 (2020), arXiv:2001.08790 [astro-ph.GA].
- [125] S. M. Koushiappas and A. Loeb, *Phys. Rev. Lett.* **119**, 041102 (2017), arXiv:1704.01668 [astro-ph.GA].
- [126] A. Gervois and H. Navelet, *Journal of Mathematical Physics* **26**, 633 (1985).
- [127] DLMF, “NIST Digital Library of Mathematical Functions,” <http://dlmf.nist.gov/> (2019), release 1.0.24 of 2019-09-15, F. W. J. Olver, A. B. Olde Daalhuis, D. W. Lozier, B. I. Schneider, R. F. Boisvert, C. W. Clark, B. R. Miller, B. V. Saunders, H. S. Cohl, and M. A. McClain, eds.
- [128] W. N. Bailey, *Proceedings of the London Mathematical Society* **s2-40**, 37 (1936).
- [129] J.-O. Gong, *JCAP* **07**, 022 (2014), arXiv:1403.5163 [astro-ph.CO].
- [130] S. Mukohyama, R. Namba, M. Peloso, and G. Shiu, *JCAP* **08**, 036 (2014), arXiv:1405.0346 [astro-ph.CO].
- [131] N. Aghanim *et al.* (Planck), *Astron. Astrophys.* **641**, A6 (2020), arXiv:1807.06209 [astro-ph.CO].
- [132] M. Kawasaki, N. Kitajima, and T. T. Yanagida, *Phys. Rev. D* **87**, 063519 (2013), arXiv:1207.2550 [hep-ph].
- [133] C. Caprini and D. G. Figueroa, *Class. Quant. Grav.* **35**, 163001 (2018), arXiv:1801.04268 [astro-ph.CO].

- [134] L. A. Boyle and A. Buonanno, *Phys. Rev. D* **78**, 043531 (2008), [arXiv:0708.2279 \[astro-ph\]](#).
- [135] B. Allen and J. D. Romano, *Phys. Rev. D* **59**, 102001 (1999), [arXiv:gr-qc/9710117](#).
- [136] T. L. Smith, E. Pierpaoli, and M. Kamionkowski, *Phys. Rev. Lett.* **97**, 021301 (2006), [arXiv:astro-ph/0603144](#).
- [137] E. Aver, K. A. Olive, and E. D. Skillman, *JCAP* **07**, 011 (2015), [arXiv:1503.08146 \[astro-ph.CO\]](#).
- [138] R. J. Cooke, M. Pettini, and C. C. Steidel, *Astrophys. J.* **855**, 102 (2018), [arXiv:1710.11129 \[astro-ph.CO\]](#).
- [139] S. Vagnozzi, *Phys. Rev. D* **102**, 023518 (2020), [arXiv:1907.07569 \[astro-ph.CO\]](#).
- [140] T. Hsyu, R. J. Cooke, J. X. Prochaska, and M. Bolte, *Astrophys. J.* **896**, 77 (2020), [arXiv:2005.12290 \[astro-ph.GA\]](#).
- [141] S. Aiola *et al.* (ACT), *JCAP* **12**, 047 (2020), [arXiv:2007.07288 \[astro-ph.CO\]](#).
- [142] V. Mossa *et al.*, *Nature* **587**, 210 (2020).
- [143] O. Farooq, R. Zahoor, and B. Francis, . (2025), [arXiv:2502.05194 \[astro-ph.CO\]](#).
- [144] A. M. Green, A. R. Liddle, K. A. Malik, and M. Sasaki, *Phys. Rev. D* **70**, 041502 (2004), [arXiv:astro-ph/0403181](#).
- [145] A. Katz, J. Kopp, S. Sibiryakov, and W. Xue, *JCAP* **12**, 005 (2018), [arXiv:1807.11495 \[astro-ph.CO\]](#).
- [146] P. Montero-Camacho, X. Fang, G. Vasquez, M. Silva, and C. M. Hirata, *JCAP* **08**, 031 (2019), [arXiv:1906.05950 \[astro-ph.CO\]](#).
- [147] A. Arbey, J. Auffinger, and J. Silk, *Phys. Rev. D* **101**, 023010 (2020), [arXiv:1906.04750 \[astro-ph.CO\]](#).
- [148] M. Boudaud and M. Cirelli, *Phys. Rev. Lett.* **122**, 041104 (2019), [arXiv:1807.03075 \[astro-ph.HE\]](#).
- [149] W. DeRocco and P. W. Graham, *Phys. Rev. Lett.* **123**, 251102 (2019), [arXiv:1906.07740 \[astro-ph.CO\]](#).
- [150] R. Laha, J. B. Muñoz, and T. R. Slatyer, *Phys. Rev. D* **101**, 123514 (2020), [arXiv:2004.00627 \[astro-ph.CO\]](#).
- [151] G. Ballesteros, J. Coronado-Blázquez, and D. Gaggero, *Phys. Lett. B* **808**, 135624 (2020), [arXiv:1906.10113 \[astro-ph.CO\]](#).
- [152] R. Laha, *Phys. Rev. Lett.* **123**, 251101 (2019), [arXiv:1906.09994 \[astro-ph.HE\]](#).
- [153] H. Poulter, Y. Ali-Haïmoud, J. Hamann, M. White, and A. G. Williams, . (2019), [arXiv:1907.06485 \[astro-ph.CO\]](#).
- [154] K. Tokeshi, K. Inomata, and J. Yokoyama, *JCAP* **12**, 038 (2020), [arXiv:2005.07153 \[astro-ph.CO\]](#).
- [155] K. Inomata, M. Kawasaki, K. Mukaida, and T. T. Yanagida, *Phys. Rev. D* **97**, 043514 (2018), [arXiv:1711.06129 \[astro-ph.CO\]](#).
- [156] A. Mitridate, D. Wright, R. von Eckardstein, T. Schröder, J. Nay, K. Olum, K. Schmitz, and T. Trickle, . (2023), [arXiv:2306.16377 \[hep-ph\]](#).
- [157] A. Lewis, . (2019), [arXiv:1910.13970 \[astro-ph.IM\]](#).
- [158] B. Dasgupta, R. Laha, and A. Ray, *Phys. Rev. Lett.* **125**, 101101 (2020), [arXiv:1912.01014 \[hep-ph\]](#).
- [159] R. Laha, P. Lu, and V. Takhistov, *Phys. Lett. B* **820**, 136459 (2021), [arXiv:2009.11837 \[astro-ph.CO\]](#).
- [160] K. Ando, K. Inomata, and M. Kawasaki, *Phys. Rev. D* **97**, 103528 (2018), [arXiv:1802.06393 \[astro-ph.CO\]](#).
- [161] S. Young, *Int. J. Mod. Phys. D* **29**, 2030002 (2019), [arXiv:1905.01230 \[astro-ph.CO\]](#).
- [162] I. Musco, K. Jedamzik, and S. Young, *Phys. Rev. D* **109**, 083506 (2024), [arXiv:2303.07980 \[astro-ph.CO\]](#).
- [163] S. Young, *JCAP* **05**, 037 (2022), [arXiv:2201.13345 \[astro-ph.CO\]](#).
- [164] S. Young and M. Musso, *JCAP* **11**, 022 (2020), [arXiv:2001.06469 \[astro-ph.CO\]](#).
- [165] S. Young, I. Musco, and C. T. Byrnes, *JCAP* **11**, 012 (2019), [arXiv:1904.00984 \[astro-ph.CO\]](#).
- [166] V. De Luca, G. Franciolini, A. Kehagias, M. Peloso, A. Riotto, and C. Únal, *JCAP* **07**, 048 (2019), [arXiv:1904.00970 \[astro-ph.CO\]](#).
- [167] M. Shiraishi, *Front. Astron. Space Sci.* **6**, 49 (2019), [arXiv:1905.12485 \[astro-ph.CO\]](#).
- [168] Z.-Z. Peng, Y. Wu, and L. Liu, *Phys. Rev. D* **111**, 103506 (2025), [arXiv:2412.19196 \[astro-ph.CO\]](#).

Supplemental Material

This supplemental material contains more details on the evolution of total density power spectrum and full constraints on model parameters.

I. EVOLUTION OF DENSITY POWER SPECTRUM

The total density contrast δ up to the second order is given as

$$\delta(k, \eta) = \delta_{\mathbf{k}}^{(1)}(x) + \delta_{\mathbf{k}}^{(2)}(x) \equiv \frac{4}{9} \frac{k^2}{\mathcal{H}^2} T(x) \zeta_k^{(1)} + \delta_{\mathbf{k}}^{(2)}(x) \quad (\text{S.1})$$

It is straightforward to derive the power spectrum by calculating the 2-point correlators as defined in main text. The total power spectrum of density perturbations is expressed as following

$$\mathcal{P}_\delta(k, \eta) = \left(\frac{k}{\mathcal{H}}\right)^4 \mathcal{P}_\zeta + \mathcal{P}_{\delta^{(2)}}(k, \eta) \equiv A_s \left(\frac{k}{\mathcal{H}}\right)^4 \left(\frac{k}{k_s}\right)^{n_s-1} + \mathcal{P}_{\delta^{(2)}}(k, \eta) \quad (\text{S.2})$$

A. Power-Law Spectrum:

For the total power-law spectrum, the second-order density power spectrum is simplified as following:

$$\mathcal{P}_{\delta^{(2)}}^{\text{PL}}(k) \simeq \frac{1}{2} A_s^2 r^2 \left(\frac{k}{k_s}\right)^{2n_t} \int_0^\infty \int_{|1-v|}^{1+v} f(u, v) \overline{\mathcal{I}^2(u, v)} (uv)^{n_t-3} \equiv A_s^2 Q(n_t, r) \left(\frac{k}{k_s}\right)^{2n_t} \quad (\text{S.3})$$

n_t	1.0	1.375	1.75	2.125	2.5
r	10^{-3}	10^{-6}	10^{-9}	1×10^{-12}	10^{-15}
$Q(n_t, r)$	385.15	193.03	8587.20	824122.921	91501961.32

TABLE S.I. The coefficient $Q(n_t, r)$ estimated from the numerical integral for different values of n_t and r .

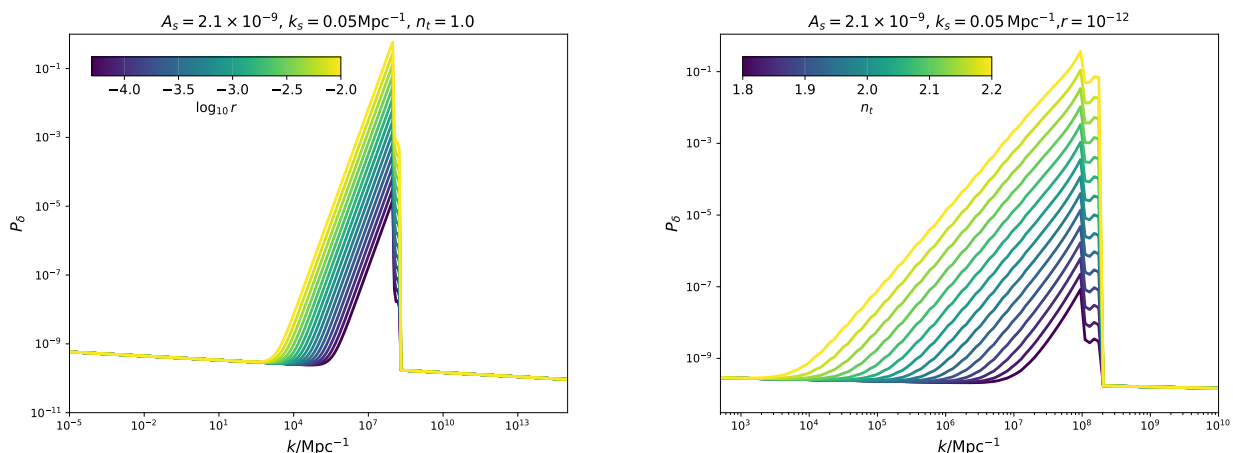


FIG. S.1. Evolution of total density power spectrum for Power-law type spectrum. We have numerically integrated Eq. (S.3) using the expression given in Eq. (11) (see main text). Due to the Heaviside function, we note that slope of the resulting expression differs from exact result slightly around its peak. We have fixed the scalar power spectrum parameters $A_s = 2.1 \times 10^{-9}$, $k_s = 0.05 \text{ Mpc}^{-1}$, and $n_s = 0.96$ according to CMB measurements [131]. We fix the tensor spectral index $n_t = 1.0$ and vary to tensor-to-scalar ratio $r \in [10^{-5}, 10^{-2}]$ in left panel and vary $n_t \in [1.8, 2.2]$ and $r = 10^{-12}$ in right panel.

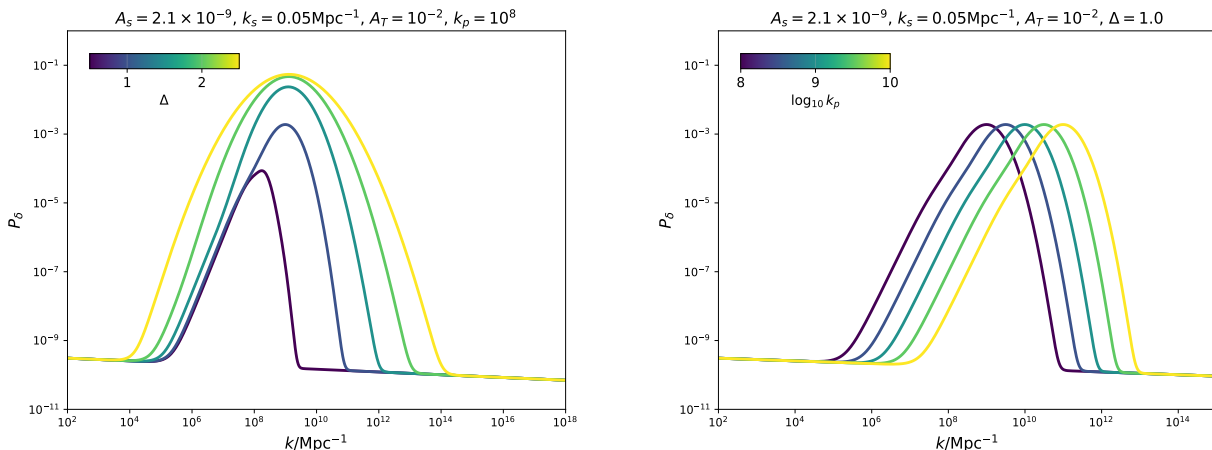


FIG. S.2. Evolution of total density power spectrum for Log-Normal type spectrum. We show the impact of the spectrum width Δ and peak frequency k_p on the total power spectrum in left and right panel respectively. Note that for $\Delta = 0.5$ the spectrum shows the similar slope as in Eq. (S.6).

B. Log-Normal Spectrum:

For the Log-Normal spectrum, the analytical solution can be found for $\Delta \rightarrow 0$. In this limit, LN power spectrum reduces to Dirac-Delta power spectrum and its analytical solution can be expressed as:

$$\mathcal{P}_{\delta^{(2)}}^{\text{LN}}(k) \stackrel{\Delta \rightarrow 0}{\simeq} \frac{1}{2} \left(\frac{k}{k_p} \right)^4 f \left(\frac{k_p}{k}, \frac{k_p}{k} \right) \overline{\mathcal{I}^2 \left(\frac{k_p}{k}, \frac{k_p}{k} \right)} \quad (\text{S.4})$$

where $f(u, v)$ is the contraction of polarization tensor calculated as following:

$$f(u, v) = \frac{1}{16 u^4 v^4} \left\{ v^8 + (u^2 - 1)^4 + 4v^6 (7u^2 - 1) + 4v^2 (u^2 - 1)^2 (7u^2 - 1) + v^4 (6 - 60u^2 + 70u^4) \right\}. \quad (\text{S.5})$$

It is important to investigate the infrared tail of induced density power spectrum in Eq. (S.4) as it provides the growth of the spectrum and plays an important role in formation of PBH formation. Infrared scales corresponds to $k \gg k_p$ and in such limit the spectrum reduces to the following:

$$\mathcal{P}_{\delta^{(2)}}^{\text{LN}}(k \ll k_p) \stackrel{\Delta \rightarrow 0}{\simeq} \frac{1}{\pi^3} \left(\frac{k}{k_p} \right)^4 \left[6 \left(\frac{k_p}{k} \right)^2 - 4 \log \left(\frac{k_p}{k} \right) - 3 \right] \quad (\text{S.6})$$

It is clear from Eq. (S.6), the induced power spectrum $\mathcal{P}_{\delta^{(2)}}^{\text{LN}} \propto k^4$ with a peak situated around $k/k_p \approx \sqrt{3}$.

II. RESULTS FOR PGW ENERGY SPECTRUM FROM NANOGrAV AND PTA

In the main text, we show the two dimensional contour plots for relevant model parameters. In this section, we detail the observational data and present the full posterior distributions. The NANOGrav data set measures the characteristic strain across 15 frequency bins spanning $f \in [2 \times 10^{-9}, 6 \times 10^{-8}]$ Hz, while the EPTA DR2 data provides measurements in 9 bins covering $f \in [3.0 \times 10^{-9}, 2.8 \times 10^{-8}]$ Hz. We use PTArcade in ceffyl modes to generate the chains for both data individually. After generating the posterior chains, we perform the KDE to jointly analyze both measurements. We provide the triangle plots for model parameters obtained from the analysis of NANOGrav 15 and EPTA DR2 data. In the left panel of Fig. S.3 and Fig. 1 (main text), we use a derived parameter defined as gravitational wave energy density evaluated at reference frequency $f_{\text{yr}} (= 1 \text{ yr}^{-1} \approx 3.17 \times 10^{-8} \text{ Hz})$ given as

$$h^2 \Omega_{\text{GW}}(f) = 1.19 \times 10^{-16} \left(\frac{r}{0.032} \right) \left(\frac{A_s}{2.1 \times 10^{-9}} \right) \left(\frac{f}{f_s} \right)^{n_t}, \quad (\text{S.7})$$

with $f_s = 8 \times 10^{-17} \text{ Hz}$ is frequency corresponding to the CMB pivot scale.

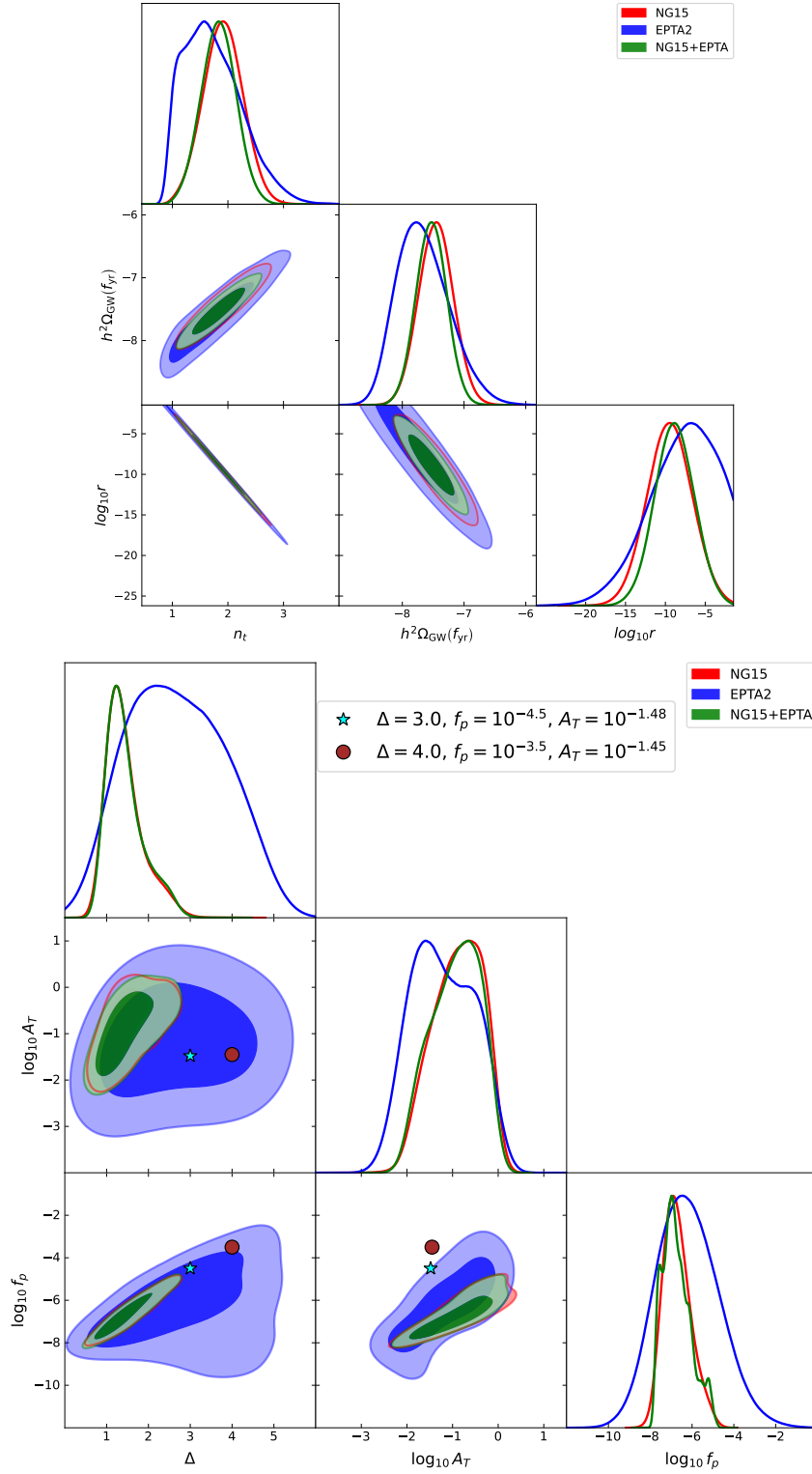


FIG. S.3. Triangle plot for posterior distribution for PL (top) and LN (bottom) spectrum. Note that $\Omega_{\text{GW}}(f_{\text{yr}})$ is a derived quantity derived using the posterior values for $\log_{10} r$ and n_t . The brown and cyan points corresponds to PBHs with mass function dominated at $10^{-12} M_{\odot}$ and $10^{-10} M_{\odot}$ shown in main text.